GEOPHYSICS, VOL. 75, NO. 4 (JULY-AUGUST 2010); P. D27–D36, 16 FIGS.
10.1190/1.3453416

Building tilted transversely isotropic depth models using localized anisotropic tomography with well information

Andrey Bakulin[2], Marta Woodward[1], Dave Nichols[1], Konstantin Osypov[1], and Olga Zdraveva[1]

ABSTRACT

Tilted transverse isotropy (TTI) is increasingly recognized as a more geologically plausible description of anisotropy in sedimentary formations than vertical transverse isotropy (VTI). Although model-building approaches for VTI media are well understood, similar approaches for TTI media are in their infancy, even when the symmetry-axis direction is assumed known. We describe a tomographic approach that builds localized anisotropic models by jointly inverting surface-seismic and well data. We present a synthetic data example of anisotropic tomography applied to a layered TTI model with a symmetry-axis tilt of 45 degrees. We demonstrate three scenarios for constraining the solution. In the first scenario, velocity along the symmetry axis is known and tomography inverts for Thomsen's ε and δ parameters. In the second scenario, tomography inverts for ε, δ, and velocity, using surface-seismic data and vertical check-shot traveltimes. In contrast to the VTI case, both these inversions are nonunique. To combat nonuniqueness, in the third scenario, we supplement check-shot and seismic data with the δ profile from an offset well. This allows recovery of the correct profiles for velocity along the symmetry axis and ε. We conclude that TTI is more ambiguous than VTI for model building. Additional well data or rock-physics assumptions may be required to constrain the tomography and arrive at geologically plausible TTI models. Furthermore, we demonstrate that VTI models with atypical Thomsen parameters can also fit the same joint seismic and check-shot data set. In this case, although imaging with VTI models can focus the TTI data and match vertical event depths, it leads to substantial lateral mispositioning of the reflections.

INTRODUCTION

Vertical transverse isotropy (VTI) is a useful approximation to describe anisotropic subsurface formations. However, widespread application of VTI depth imaging often suggests that the direction of the symmetry axis may not be vertical. Indeed, if sedimentary formations were deposited in a layer-cake geometry and later folded by tectonic forces, then tilted transverse isotropy (TTI) with the axis perpendicular to the bedding plane might be a more appropriate description. Such media are sometimes referred to as demonstrating structurally conformant transverse isotropy (Audebert et al., 2006). However, in an alternative geologic scenario, tectonic action and deposition may occur together, and the symmetry axis may no longer be perpendicular to the bedding plane. In yet another scenario, sediments may be subjected to anomalous stresses around salt bodies, which can result in stress-induced anisotropy (Sengupta et al., 2009). In this case, because symmetry is controlled by principal stress directions that are not vertical, horizontal, or perpendicular to the bedding axis, general TTI or even an orthorhombic medium is expected.

For any of these scenarios, we should be able to build an anisotropic model for depth imaging that is governed by a geologically plausible anisotropic velocity field. In practical circumstances, this usually requires supplementing seismic data with some kind of well information (Bear et al., 2005). For a VTI case, constraining vertical well data in the form of a check-shot survey or depth markers usually resolves the existing ambiguity (around the well) and delivers a unique depth model that fits all of the data. Therefore, it has become common industry practice to estimate anisotropic parameters with the aid of borehole information (Sexton and Williamson, 1998; Tsvankin, 2001; Morice et al., 2004; Bear et al., 2005; Huang et al., 2007).

The information content of the well and seismic data is well understood for layered VTI models, and, from this case, most ap-

Presented at the 79th Annual International Meeting, Society of Exploration Geophysicists.
Manuscript received by the Editor 31 December 2009; revised manuscript received 24 February 2010; published online 2 August 2010.
[1]WesternGeco/Schlumberger, Houston, Texas, U.S.A. E-mail: woodward2@slb.com; nichols0@slb.com; kosypov@slb.com; ozdraveva@slb.com.
[2]Formerly WesternGeco/Schlumberger; presently Saudi Aramco, Dhahran, Saudi Arabia. E-mail: andrey.bakulin@aramco.com.

proaches and physical intuition originate. However, for TTI models, such a practical foundation has not been established, even though an analytical description of various seismic signatures for TTI media is available (Tsvankin, 2001). Figure 1 shows some typical practical scenarios where dipping sediment layers may require a TTI description. It is imperative that we be able to calibrate our models and estimate TTI parameters in the presence of complex structures. In addition, well data often come from deviated boreholes, thus requiring a calibration method to handle this additional complexity.

Bakulin et al. (2009a) propose using conventional gridded reflection tomography to invert seismic and well data jointly for a local anisotropic VTI depth model. We extend this technique to TTI media and attempt to answer two questions:

1) Is it feasible to invert for a local TTI model using certain combinations of seismic and well data?
2) Can we distinguish TTI and VTI models using a joint seismic and well data set alone?

The answers obviously depend on the model geometry. Therefore, we focus on the simplest case of a layered model where we can determine analytically if the inverse problem is unique and which parameters can be estimated. We start by describing the approach of localized gridded anisotropic tomography that inverts a joint seismic and well data set. Then we apply it to a synthetic example where we build a local TTI model. We observe some ambiguities and explain them with an analytical description of seismic signatures. Next, we build a VTI model that fits the same data set and explain why this does not lead to obvious contradictions. At the end, we discuss the implications of imaging a TTI subsurface with a VTI velocity model.

LOCALIZED REFLECTION TOMOGRAPHY

Postmigration anisotropic gridded reflection tomography of surface seismic data is a well-established tool to build velocity models in depth (Woodward et al., 1998, 2008; Zhou et al., 2004). For borehole data, anisotropic traveltime tomography in the premigrated domain is a more typical model-building approach (Chapman and Pratt, 1992; Pratt and Chapman, 1992). Common industry practice uses reflection tomography to build anisotropic velocity models. However, typically we only invert for velocity along the symmetry axis; the remaining anisotropic velocity field parameters are kept fixed. They are derived beforehand using manual well calibrations, regional trends, or other nontomographic methods.

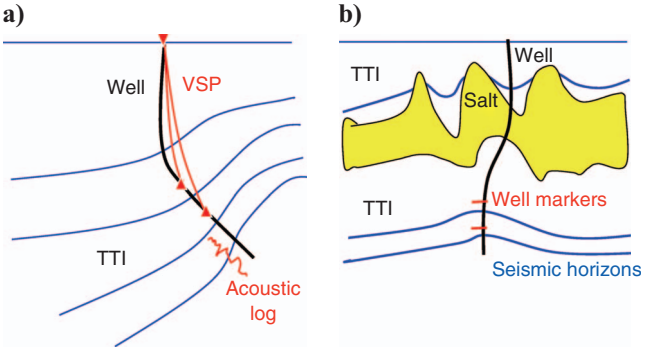

Figure 1. Sketch of various scenarios that involve a complex subsurface and deviated wells, which would require estimation of TTI parameters aided by well information: (a) sediment anticline; (b) subsalt targets.

In the case of VTI media, Thomsen parameters ε and δ can be derived near a well location using a manual layer-stripping approach, provided the seismic data are supplemented by check-shot or marker information. Then, such parameters are propagated into a volume using geologic horizons as a guide. In the case of TTI media, two additional parameters such as tilt and azimuth of the symmetry axis are often derived from the seismic dip field under the assumption that the symmetry axis is perpendicular to the geologic beds (Audebert et al., 2006) or some other simple geometric relationships. Such practices stem from an understanding that inverting simultaneously for several parameters of the anisotropic velocity field is almost always an underconstrained problem when seismic data alone are used (Tsvankin, 2001).

Quite simply, we must acknowledge that it is impossible to derive anisotropic parameters away from well control using seismic data alone. As a result, practical focus shifts toward designing techniques that estimate anisotropic parameters with the help of well data. Various methods have been proposed to handle this problem (Tsvankin, 2001; Morice et al., 2004; Bear et al., 2005; Huang et al., 2007; Wang and Tsvankin, 2009); however, most of them are designed for vertical wells and VTI media. In addition, most of them do not easily relate to the common postmigration approaches used for conventional model building. Although manual 1D layer-stripping inversion by Morice et al. (2004) and 1D joint inversion by Huang et al. (2007) use prestack depth-migrated data, they still apply only to VTI media with flat layers. Therefore, most existing approaches cannot be used for anisotropic calibration in the typical 3D scenarios shown in Figure 1.

Bakulin et al. (2009a) propose using localized multiparameter joint inversion of seismic and well data using conventional gridded reflection tomography. Multiparameter inversion becomes constrained and feasible under three conditions:

1) The seismic data set is inverted jointly with one or more types of well data (velocity measured in wells, traveltimes measured from check shot or vertical seismic profiling [VSP], markers, or other).
2) The inversion is performed in a local volume around the well where well data are assumed to remain valid.

We must emphasize that independent inversion for multiple parameters at each grid cell away from the well is highly nonunique. Therefore, we add a shape constraint to the parameter update by using preconditioning to smooth and steer the solution along geological layers away from the well. This strategy prevents uncontrolled lateral variation of the anisotropic parameters that would make the inverse problem highly unstable. There are multiple practical advantages to using conventional reflection tomography for simultaneous joint inversion. The most important is that the constraints can be introduced in a flexible way using the same gridded model without the need to rebuild or regrid the model every iteration, as is the requirement in many other sequential techniques.

SYNTHETIC EXAMPLE

Let us apply anisotropic tomography with well constraints to a simple deepwater model. The subsurface is represented by layered TTI sediment with a uniform symmetry-axis tilt of 45° (Figure 2). The model has smooth vertical variation of velocity and anisotropy. Two pronounced velocity inversions are present in the model. They are also accompanied by anisotropy reductions. A cable length of 12 km is assumed. A prestack gather computed with anisotropic ray tracing is shown in Figure 2c. Reflected events from 49 density-contrast interfaces are located every 200 m.

We assume a certain orientation of the symmetry axis and apply anisotropic reflection tomography (Woodward et al., 2008) to solve for a local anisotropic model using joint inversion of seismic and well data. Well data may come in various forms, but in this study we only examine velocity measured along the well (acoustic log) or check-shot survey. We apply a mute of 50° to the data before inversion. This limits the useable offsets to less than 8 km for events above 6 km; however, even with a maximum offset of 12 km, half-opening angles remain less than 40° for events deeper than 8 km.

First, we attempt to build a TTI velocity model assuming that the true orientation of the symmetry axis is known. Second, we attempt a VTI inversion of the seismic and check-shot data, pretending that the symmetry axis is vertical. In each case, we benchmark tomographic results against an analytic description of seismic signatures and validate the results. Finally, we contrast TTI and VTI results and highlight the consequences of replacing TTI media with VTI media.

BUILDING A LOCAL TTI MODEL

It is a common practice not to invert for orientation of the symmetry axis. Let us assume that the true orientation is known and fixed. Under this assumption, we proceed with building the local TTI model using seismic and well data. We consider three different scenarios for the well data:

1) accurate knowledge of symmetry-axis P-wave velocity V_{P0} derived from an acoustic log in a deviated well, a virtual check shot, or an offset well
2) check-shot survey in a vertical well
3) check-shot survey in a vertical well and correct profile of Thomsen's δ from an offset well.

First, we present the tomographic results for all three scenarios. Then we attempt to explain them using theoretical analysis and discuss the differences between these scenarios.

Two-parameter inversion after fixing V_{P0}

Let us assume that well data are available from a deviated well drilled along the TTI symmetry axis (45° to the vertical in our case). Velocity along the well can be estimated from acoustic logs or by performing virtual check shots (Mateeva et al., 2006). Alternatively, one may utilize a V_{P0} profile derived with the help of an offset well. After fixing V_{P0} to its correct values, we attempt tomographic reconstruction of δ and ε from long-offset reflection seismic data. Although such an inversion would be unique and stable for the VTI case, for this TTI case only an approximate model is recovered (Figure 3). Individual values of the Thomsen parameters (δ in particular) show errors of 0.05 and more. Nevertheless, the final model provides image gathers that appear as flat as in the true model (Figure 10b).

Three-parameter inversion of seismic and vertical check-shot data

In the second scenario, we assume the availability of a vertical well with a check-shot survey acquired every 50 m from 1.5 to 11 km. We jointly invert seismic and check-shot data for three parameters (V_{P0}, ε, and δ) around the well. Because we have long-spread data, such an inversion would result in a unique recovery of the true model in a VTI case. To our surprise, TTI inversion leads to a different model (Figure 4) that provides a reasonable fit to the check-shot survey (Figure 5) and that flattens the image gathers but that has geologically implausible ε and δ profiles.

It may seem that the unfortunate model we arrived at is caused by the poor initial guess of anisotropy. To investigate it further, let us repeat the same inversion but start with a much better initial model that has $\varepsilon = 0.08$ and $\delta = 0.03$. In this case, we again can easily match all of the data and this time arrive at a model with positive Thomsen parameters; however, this model is still quite far removed from the true one (Figure 6). These results suggest deeper underlying reasons for the observed ambiguity.

Two-parameter inversion of seismic and vertical check-shot data after fixing the correct profile of Thomsen's δ from an offset well

In the third scenario, we supplement the vertical check shot with knowledge of the correct profile of δ from an offset well. Tomography performs a two-parameter inversion (V_{P0} and ε) of the seismic and check-shot data and recovers excellent estimates of the unknown parameters at all depths (Figure 7).

Weak-anisotropy analysis of the results

Why do such different models provide similar fits to this seemingly complete data set? To obtain analytical insight into the problem, it is instructive to obtain weak-anisotropy expressions for all P-wave TTI signatures at hand. For a single horizontal TTI layer with a 45° symmetry-axis tilt, these signatures are expressed as follows (Tsvankin, 2001; Pech et al., 2003):

$$V_{\mathrm{NMO}}^{\mathrm{TTI}} = V_{\mathrm{P0}}^{\mathrm{TTI}}(1 + 1.25\varepsilon^{\mathrm{TTI}} - 0.75\delta^{\mathrm{TTI}}), \tag{1}$$

$$V_{v}^{\mathrm{TTI}} = V_{\mathrm{P0}}^{\mathrm{TTI}}[1 + 0.25(\varepsilon^{\mathrm{TTI}} + \delta^{\mathrm{TTI}})], \tag{2}$$

$$A_4 = \frac{2\eta^{\mathrm{TTI}}}{t_{\mathrm{P0}}^2 (V_{\mathrm{P0}}^{\mathrm{TTI}})^4}. \tag{3}$$

Here, $V_{\mathrm{P0}}^{\mathrm{TTI}}$, δ^{TTI}, and $\varepsilon^{\mathrm{TTI}}$ are the three independent Thomsen parameters that describe the TTI velocity field; $\eta^{\mathrm{TTI}} \approx \varepsilon^{\mathrm{TTI}} - \delta^{\mathrm{TTI}}$; V_{v}^{TTI} denotes velocity in the true vertical direction; $V_{\mathrm{NMO}}^{\mathrm{TTI}}$ describes the normal moveout (NMO) velocity from a horizontal reflector; and A_4 is a quartic moveout coefficient describing P-wave traveltime behavior at long offsets (Tsvankin, 2001).

Various numerical coefficients arise after substituting values of zero reflector dip and tilt of the symmetry axis (45°). In the first example (Figure 3), the information constrained by the seismic data is equivalent to equations 1 and 3. Indeed, we observe that the combination $(1.25\varepsilon - 0.75\delta)$ that controls $V_{\mathrm{NMO}}^{\mathrm{TTI}}$ is best determined in Figure 3d. Parameter η^{TTI} is less well determined. This observation is analogous to a VTI case where the trade-off between V_{NMO} and A_4 leads to substantial uncertainty in the quartic coefficient and thus in

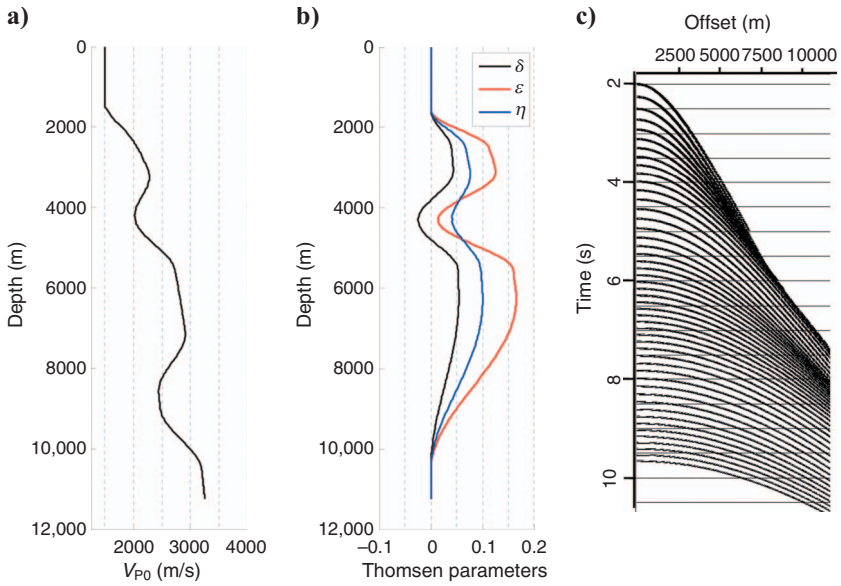

Figure 2. Deepwater horizontally layered TTI model used for tomography: (a) velocity V_{P0} (along symmetry axis, which is at 45° to the right of the downward vertical axis); (b) Thomsen parameters; (c) prestack gather. Reflections arise from 49 density interfaces. Water depth is at 1500 m.

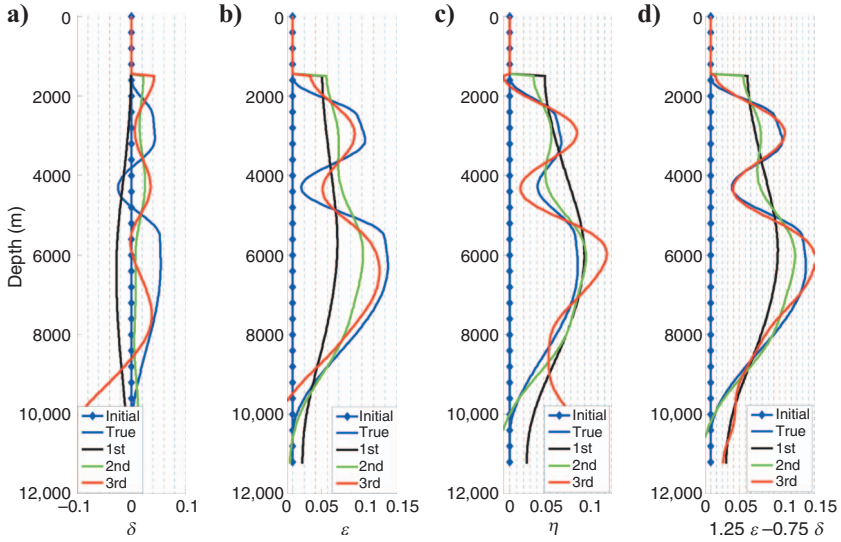

Figure 3. Results of a two-parameter TTI inversion (ε and δ) of seismic data after fixing velocity along the symmetry axis (V_{P0}). Anisotropy profiles after each iteration are shown with initial (zero) and true models: (a) δ; (b) ε; (c) η; (d) parameter combination ($1.25\varepsilon - 0.75\delta$) that controls NMO velocity (equation 1). Although this parameter combination is tightly constrained as seen in (d), δ and ε are determined with errors. In particular, δ is not well resolved.

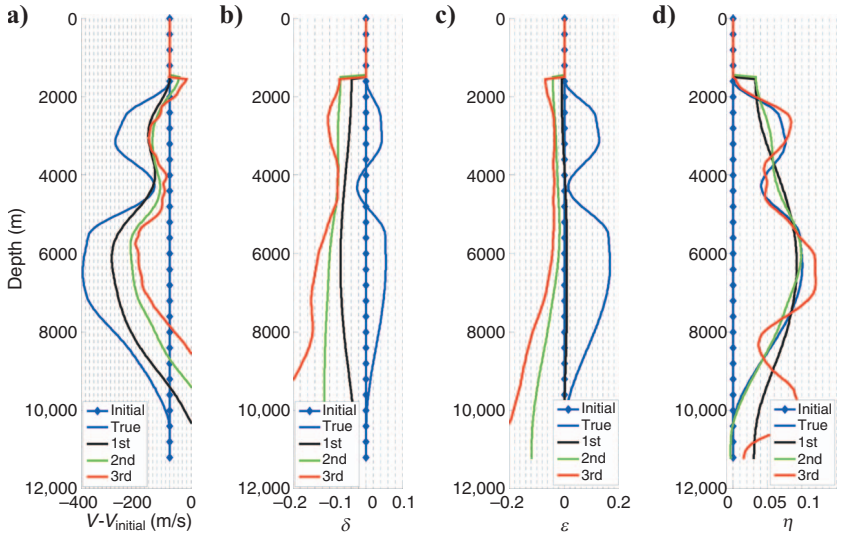

Figure 4. Results of a three-parameter TTI inversion (V_{P0}, ε, and δ) of seismic and vertical checkshot data. Velocity and anisotropy profiles after each iteration are shown with initial and true models: (a) update in velocity shown as the difference between current velocity at each iteration and initial velocity profile; (b) δ; (c) ε; (d) η. Whereas the parameter combination $\eta \cong \varepsilon - \delta$ is relatively well constrained, tomography recovers one of the equivalent models with incorrect V_{P0}, δ, and ε. In our case, η plays the same role as δ in the VTI case, relating vertical velocity and V_{NMO} according to equation 4. Even though vertical velocity V_v is constrained by the check shot, we are unable to resolve ε and δ individually because, in our case, both short- and long-spread moveouts are controlled by η (see equations 3 and 4).

η (Tsvankin, 2001). We expect the individual parameters to be less well determined because combinations $(1.25\varepsilon - 0.75\delta)$ and $(\varepsilon - \delta)$ from equations 1 and 3 are too similar to constrain them separately, thus creating additional ambiguity.

For the second case when check-shot data are available, we add information equivalent to equation 2. It is instructive to combine equations 1 and 2 and thus rewrite equation 1 in the following weak-anisotropy form:

$$V_{\mathrm{NMO}}^{\mathrm{TTI}} = V_v^{\mathrm{TTI}}(1 + \eta^{\mathrm{TTI}}). \tag{4}$$

It becomes obvious that three measurements ($V_{\mathrm{NMO}}^{\mathrm{TTI}}$, V_v^{TTI}, and A_4) do not constrain all three parameters ($V_{\mathrm{P0}}^{\mathrm{TTI}}$, $\varepsilon^{\mathrm{TTI}}$, and δ^{TTI}) because equations 4 and 3 constrain only η^{TTI}, whereas equation 2 constrains a combination of all three desired quantities. In the absence of additional information, tomography retrieves an equivalent model with correct η^{TTI} and V_v^{TTI} but incorrect individual parameters $V_{\mathrm{P0}}^{\mathrm{TTI}}$, $\varepsilon^{\mathrm{TTI}}$, and δ^{TTI}. When δ^{TTI} is additionally constrained as in the third example (Figure 5), then tomography correctly recovers $V_{\mathrm{P0}}^{\mathrm{TTI}}$ and $\varepsilon^{\mathrm{TTI}}$, as expected from the weak-anisotropy equations above.

BUILDING LOCAL VTI MODEL

Now let us assume that the true orientation of the symmetry axis is not known. We further assume that the axis of symmetry is vertical and invert vertical symmetry-axis velocity directly from check-shot traveltimes recorded in a vertical well. After fixing the vertical velocity, we perform a two-parameter inversion (δ^{VTI} and $\varepsilon^{\mathrm{VTI}}$) of the seismic data and recover the resultant profiles (Figure 8). This solution has positive δ^{VTI} but almost zero $\varepsilon^{\mathrm{VTI}}$ and therefore negative η^{VTI}.

Weak-anisotropy analysis of VTI inversion

To understand this result, let us predict what VTI model can best fit our TTI data (Figure 9). To satisfy the same check-shot survey, we

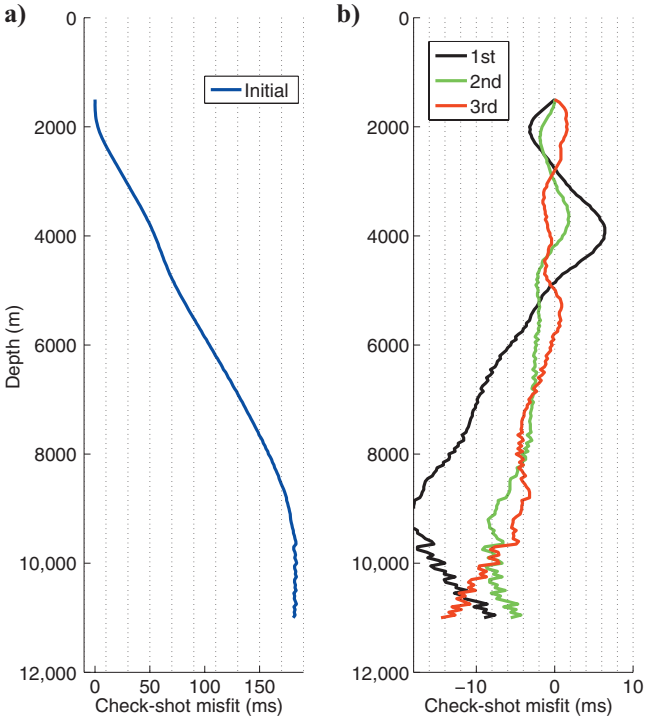

Figure 5. Misfit in check-shot traveltimes for (a) the initial model and (b) all subsequent tomography iterations for the second scenario of joint three-parameter inversion of seismic and check-shot data. Misfit is computed as the difference between experimental and predicted traveltimes.

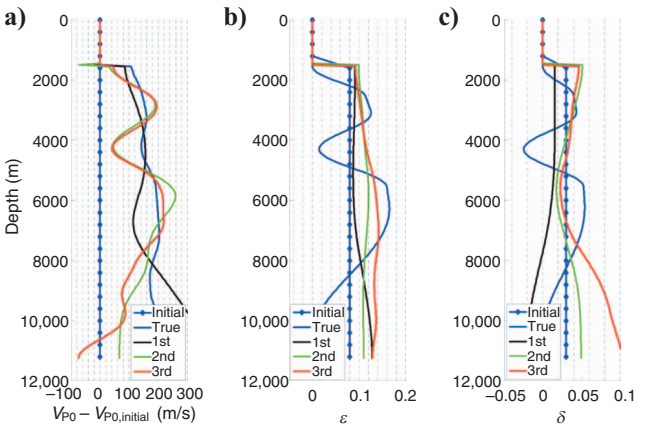

Figure 6. Same as Figure 4 but for a different initial model with $\delta = 0.03$ and $\varepsilon = 0.08$. Results of a three-parameter TTI inversion (V_{P0}, ε, and δ) of seismic and vertical check-shot data. Velocity and anisotropy profiles after each iteration are shown with initial and true models: (a) update in velocity shown as a difference between current velocity at each iteration and initial velocity profile; (b) ε; (c) δ; (d) η.

must require that $V_{P0}^{VTI} = V_v^{TTI}$. To match the same seismic data, we also require that $V_{NMO}^{VTI} = V_{NMO}^{TTI}$. Comparing normal moveout (NMO) equation 4 with the corresponding VTI equation

$$V_{NMO}^{VTI} = V_{P0}^{VTI}(1 + \delta^{VTI}), \tag{5}$$

we derive that $\delta^{VTI} = \eta^{TTI}$. Finally, we deduce that the horizontal and vertical VTI velocities must be equal to each other ($V_{P90}^{VTI} = V_{P0}^{VTI}$) to match the TTI velocity surface that is symmetric around the 45° symmetry axis (Figure 9). This implies that $\varepsilon^{VTI} = 0$. Therefore, we can conclude that the VTI medium with parameters $V_{P0}^{VTI} = V_v^{TTI}$, $\delta^{VTI} = \eta^{TTI}$, and $\varepsilon^{VTI} = 0$ has these three signatures identical to a TTI model with a 45° tilt of the symmetry axis: velocity along vertical z-axis, moveout velocity, and horizontal velocity. Profiles of the inverted parameters in Figure 8 are quite consistent with these analytical predictions, thus validating the numerical solution. These findings explain the excellent fit of the same data by TTI and VTI tomographic solutions.

DISCUSSION

Level of ambiguity in model building

As expected, all of the TTI and VTI models we derived fit the joint data set consisting of seismic and well data. Figure 10 verifies that their migrated common-image-point gathers are not only flat but

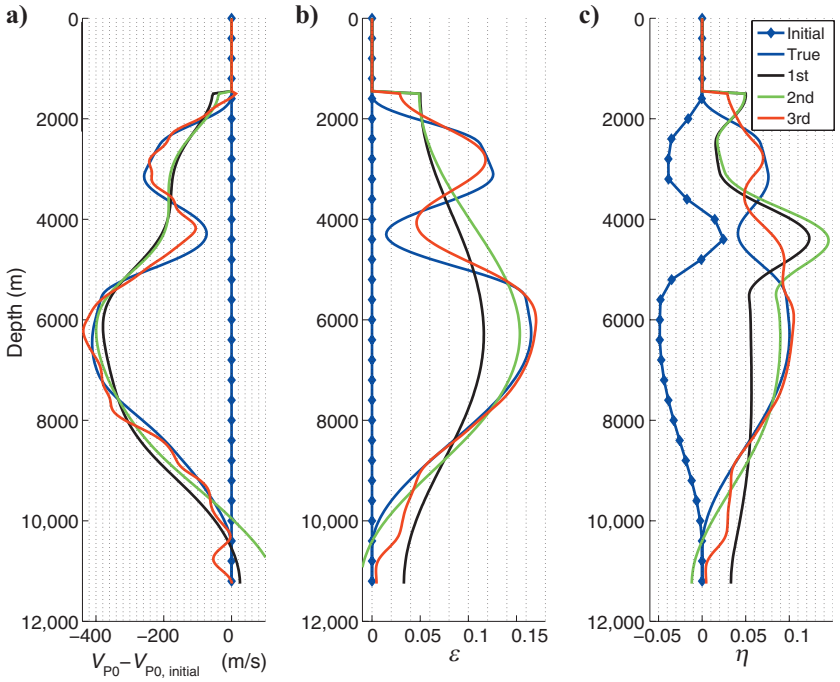

Figure 7. Results of a two-parameter TTI inversion (V_{P0} and ε) of seismic and vertical check-shot data after fixing the δ profile to true values. Velocity and anisotropy profiles after each iteration are shown with initial and true models: (a) update in velocity along symmetry axis shown as a difference between current velocity at each iteration and initial velocity profile; (b) ε; (c) η.

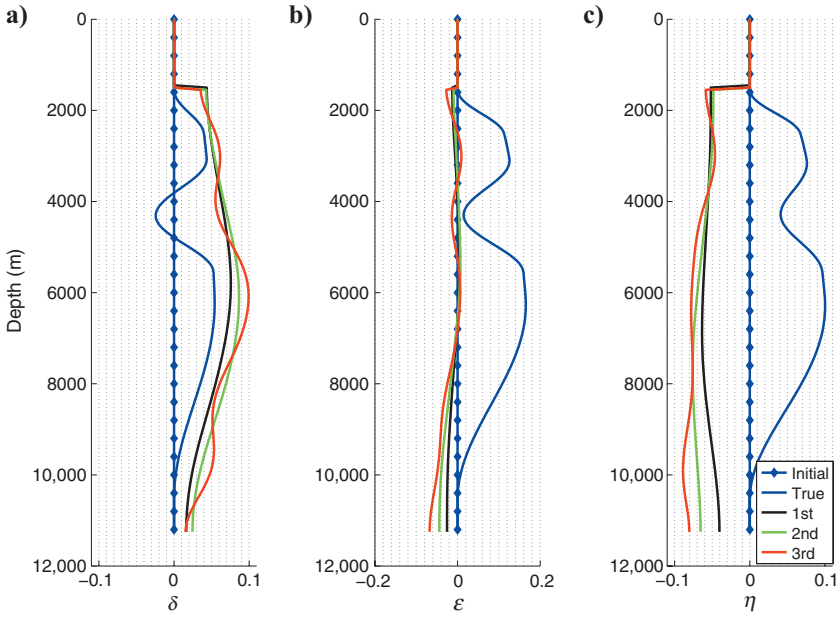

Figure 8. Results of a two-parameter inversion (ε and δ) of seismic data after assuming a VTI model and fixing vertical velocity to correct values based on the check shot. Anisotropy profiles after each iteration are shown with initial and true models: (a) δ; (b) ε; (c) η. Note that recovered δ is quite close to the true η, whereas ε is close to zero.

also have reflections positioned at the same depth with an accuracy of about 10 m. Therefore, they are indistinguishable from the focusing and vertical positioning points of view. In mathematical terms, we can say that they all are in the null space of the tomography problem.

It is further obvious from the theoretical analysis and from the variability of the TTI solutions that these are probably not the only models that fit the data. In other words, we did not fully characterize the TTI null space — we just sampled several members of a much larger set. If we were to use more sophisticated tools such as tomography with uncertainty analysis, we would be able to obtain an entire family of kinematically equivalent TTI models that make up the null space (Osypov et al., 2008; Bakulin et al., 2009b). An obvious advantage of such an approach is the ability to reveal a high level of nonuniqueness using only a single inversion. For instance, in the example of a TTI inversion of seismic and check-shot data, we easily could have detected that Thomsen parameters are not well constrained (Bakulin et al., 2009b) and then have determined additional measurements or information required to obtain a more constrained solution.

Can we distinguish TTI or VTI?

We also examined a key decision in model building: whether to use VTI or TTI parameterization. We have demonstrated on a synthetic example that, for a general TTI medium when the symmetry-axis tilt is not orthogonal to bedding, such a decision may be impossible to make based on data alone, even when well information is available. Indeed, locally, we were able to focus and correctly position seismic data in depth with either a VTI or a TTI model.

Although we have analyzed this ambiguity for a special case of 45° tilt, these conclusions should be revisited for a more general case of the symmetry-axis orientation. Does it mean we should opt for a simpler model, i.e., VTI that fits the data? The answer is a resounding "no." Good kinematic fit (data focusing) and accurate vertical positioning do not guarantee correct lateral positioning; wrongly using a VTI model that fits seismic moveout and vertical check-shot traveltimes will result in mispositioning and apparent azimuthal anisotropy. For example, if we were to image even our flat TTI data with the VTI instead of the TTI model, any amplitude anomalies along the flat reflectors would be laterally mispositioned. VTI migration of our data will always propagate energy symmetrically around a vertical reflection axis; for any offset, an image point will always fall midway between the source and receiver.

In TTI media, angles of incidence and reflection are different (Figure 11a). Therefore, TTI migration of the same data will propagate energy asymmetrically. Figure 11b quantifies the amount of this angular asymmetry as the deviation of the opening angle bisector from vertical. It is clearly controlled by local anisotropy values and can be as high as 8° (Figure 11b). Because of this asymmetry, image points are displaced to the left of their common-midpoint locations by up to 700 m (Figure 11c), which represents large lateral mispositioning from a practical standpoint.

If more complete borehole data are available, such as walkaway VSP, then VTI and TTI cases may be easily distinguished: the traveltime curve minimum in the TTI case will be shifted away from the zero-offset location.

Complexities of wave propagation in TTI models

In general, we expect more complex wave-propagation phenomena in TTI media, but in particular we want to discuss two effects that may be important for model building and imaging.

First, we want to emphasize the asymmetric propagation that we mentioned earlier. Figure 12 shows actual ray trajectories computed in our TTI model at hand from a deep reflector. One can clearly observe the effect of ray-trajectory bias to the left; in particular, one can notice that zero-offset rays are not vertical but rather are tilted to the left. This is easily explained by analyzing Snell's law in an anisotropic medium (Figure 13). By definition, zero-offset rays have zero horizontal slowness. To derive the corresponding ray direction, one must find a normal to the slowness surface (Tsvankin, 2001). Figure 13 shows that a tilted slowness surface leads to nonvertical rays, thus explaining the nonvertical zero-offset ray propagation observed in TTI media.

Second, even in a 1D layered medium, ray trajectories for a check-shot survey are not vertical, even if the well is vertical (Figure 14). As above, this deviation can be easily explained by anisotropic

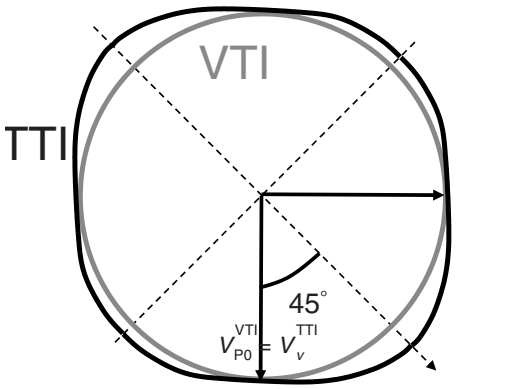

Figure 9. How to find a best-fit VTI model for a given TTI medium. A vertical cross section of the TTI phase-velocity surface (black) is symmetric around a 45° axis of symmetry. The phase velocity surface for the best-fit VTI medium (gray) matches the vertical TTI velocity in order to match the check shot. It has the same curvature near the vertical direction to match the observed NMO velocity.

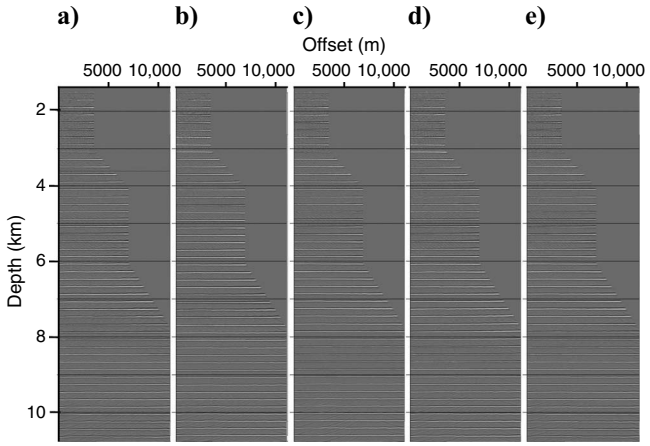

Figure 10. Common-image-point gathers for various anisotropic models derived by localized tomography: (a) true model; (b) TTI model obtained after fixing V_{P0} (see Figure 3); (c) TTI model with negative δ and ε obtained from seismic and check-shot inversion (Figure 4); (d) TTI model with positive δ and ε obtained from seismic and check-shot inversion (Figure 6); (e) VTI model.

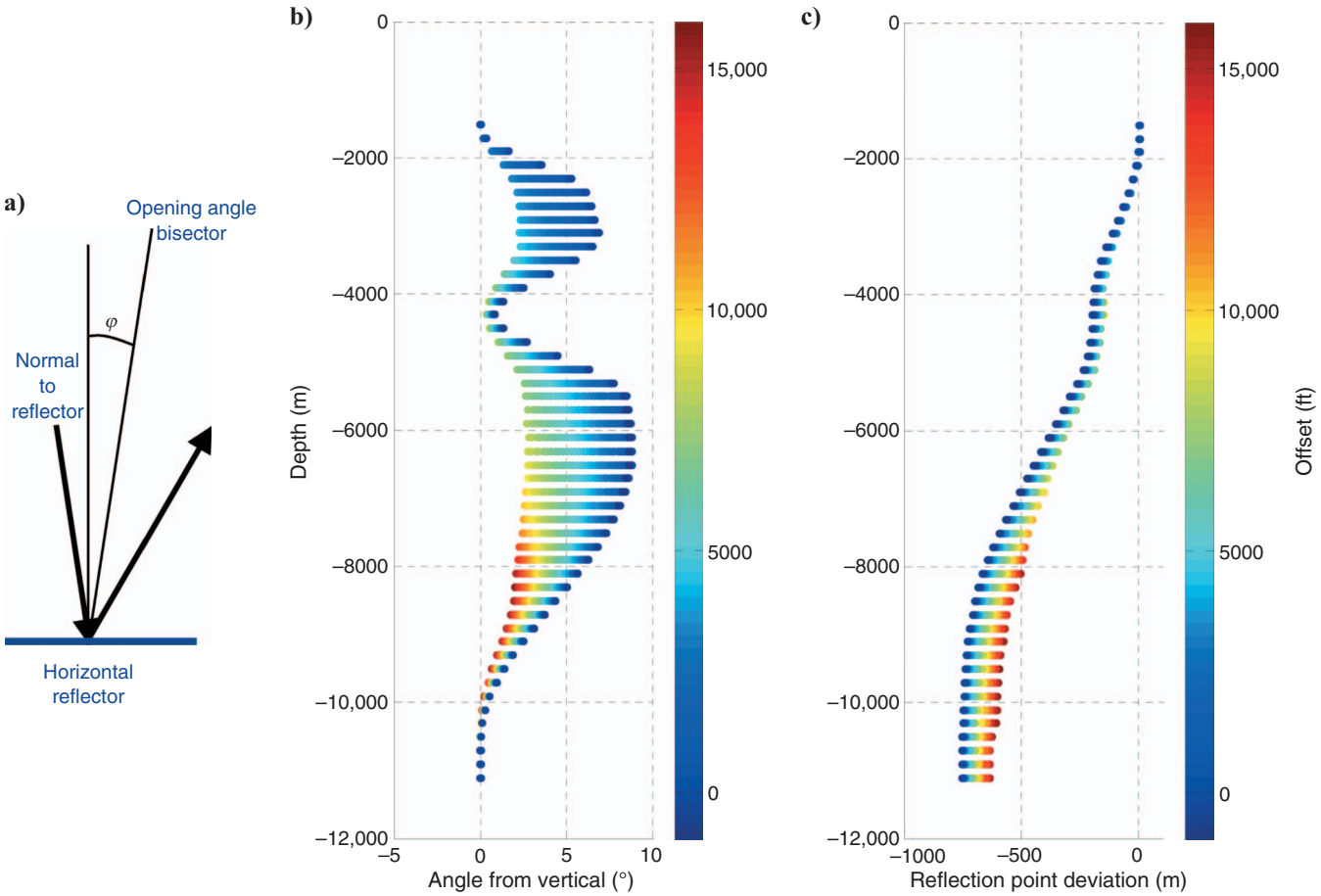

Figure 11. Location of subsurface reflection points and angles in the true TTI model as predicted by ray modeling. (a) Sketch explaining asymmetric ray propagation caused by tilt of the symmetry axis. (b) Deviation of opening angle bisector from vertical direction; angle bisector divides the opening angle between incident and reflected rays in half. For VTI media, the angle bisector is always zero, whereas for TTI media we observe a consistent shift of the angle bisector for all offsets including the zero offset. Both attributes are color coded by source-receiver offset. Observe the strong correlation between (b) and the anisotropy profiles (Figure 2). (c) Shift of actual reflection points with respect to source-receiver midpoint locations, as varying with depth and offset.

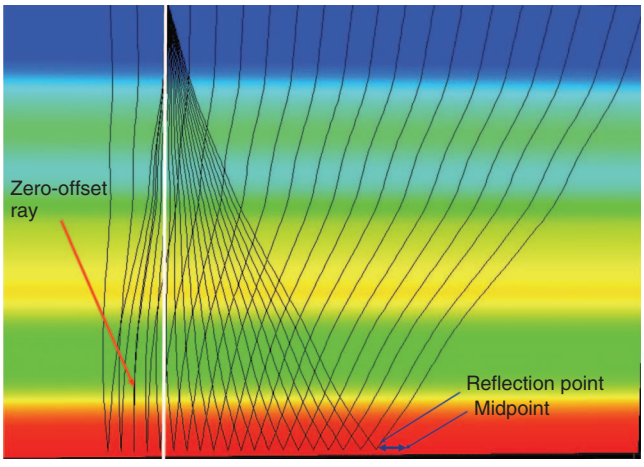

Figure 12. Ray trajectories from a deep reflector computed in the layered TTI model at hand. The zero-offset ray is not vertical, and all rays have a general bias to the left. Also, the reflection points all fall to the left of their source-receiver midpoints.

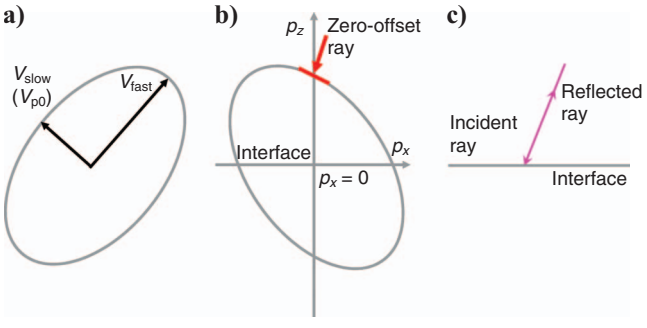

Figure 13. Schematics of Snell's law applied in a TTI medium, explaining the nonvertical nature of zero-offset rays reflecting from a horizontal reflector: (a) cross section of the phase-velocity surface; (b) cross section of the corresponding slowness curve; (c) ray diagram. For the zero-offset ray horizontal slowness (p_x) should vanish.

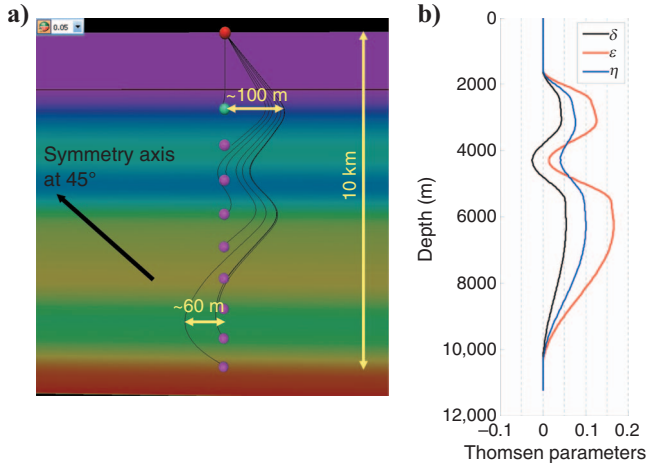

Figure 14. (a) The tilted symmetry axis in a TTI model leads to curved rays in a 1D medium with source and receiver located along a vertical borehole. (b) Deviation of the rays is controlled by the strength of the anisotropy in the model.

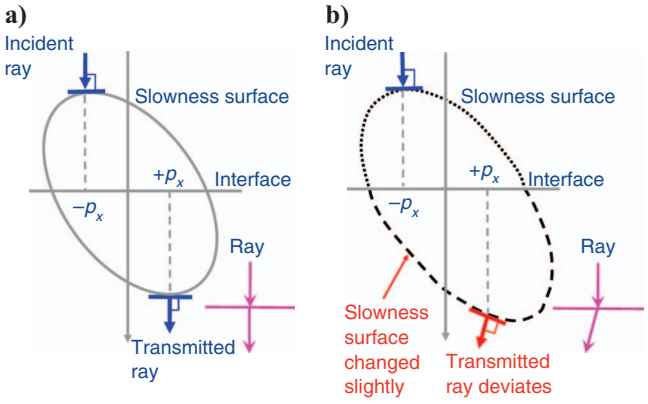

Figure 15. Snell's law diagram explains refraction of the initially vertical incident ray across the interface between two TTI media. (a) Snell's law requires preservation of horizontal slowness p_x. Thus, if two TTI media above and below are identical, then rays remain vertical. (b) A slight change in the slowness surface leads to a different normal direction for the same value of the horizontal slowness and results in a nonvertical ray after transmission.

Snell's law. If media above and below an interface are the same, then preserving horizontal slowness leads to vertical rays orthogonal to the slowness surface (Figure 15a). However, if the bottom medium changes slightly, then the tilted slowness surface deforms; for the same horizontal slowness, the ray direction becomes different, bending the initially vertical ray (Figure 15b). This is exactly what happens in our model with a tilted symmetry axis: smooth variation with depth effectively creates a set of many tiny interfaces where small bending occurs and accumulates along the ray.

Can we disregard this small effect? Although deviations out of the well may seem insignificant at first, their cumulative effect may be substantial enough to affect check-shot traveltimes computed with commonly used approximations. One of the approximations typically used is related to the perturbation technique (Červený, 2001), whereby a ray trajectory is first traced in the inhomogeneous reference isotropic medium and then traveltimes are computed using reintegration in the proper anisotropic model along this ray. If we were to apply such an approximation for computing check-shot traveltimes in our example, then the difference between true and approximate traveltimes could be as large as 12 ms at depth (Figure 16), which is enough to bias the model-building process and interpretation. From Snell's law (Figure 15) and observed trajectories (Figure 14), we can see that rays deviating from the vertical direction only occur when the symmetry axis is not orthogonal to the interface. Indeed, for horizontal reflectors in isotropic or VTI media, rays remain vertical. The amount of ray bending is likely to be proportional to the contrast in velocity and anisotropic parameters as well as the change of symmetry-axis direction across the interface (Figure 15).

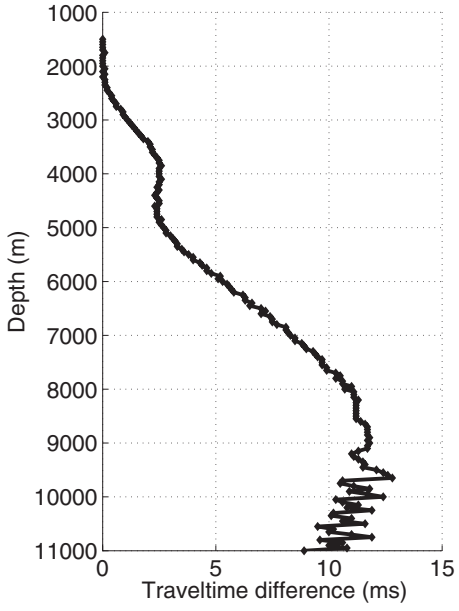

Figure 16. Traveltime difference between approximate and exact ray-traced traveltimes for a vertical check-shot survey in the TTI model of interest. Approximate times are computed using a perturbation technique of reintegrating along vertical isotropic ray trajectories.

CONCLUSIONS

We applied localized anisotropic tomography with well data to build a locally layered TTI model with a constant 45° tilt of the symmetry axis around a single borehole. In contrast to the VTI case, we observed that supplementing seismic data with velocity measured along the vertical or deviated well may still leave the problem underconstrained, even when the true orientation of the symmetry axis is known. As a result, we were able to construct several different TTI models that fit the seismic and well data, yet they were far from the correct model. In a VTI case, all such inversions would result in the true model. We were able to explain these results from first principles using weak-anisotropy approximations for reflection signatures. Because such an increased ambiguity is observed for the simplest case of layered models, we expect even more ambiguity in a 3D case. We conclude that TTI model building is more challenging than VTI model building and would likely require more well information or other constraints to arrive at a geologically plausible solution.

On the other hand, if we assume VTI symmetry, then the same data set of seismic and check-shot data can be accurately fit with a VTI model. Therefore, we demonstrated that the choice between TTI and VTI models can also be difficult. Even though both VTI and TTI models can image the data and correctly position them vertically, there are negative implications when we image TTI data with VTI models that may lead to significant lateral mispositioning.

We conclude that localized tomography which simultaneously updates velocity and Thomsen parameters should always be used with great care. Despite supplementing seismic data with well data and despite restricting the shape of the updates to geologic layers, local multiparameter inversion may still remain nonunique, as seen in the examples presented here. To arrive at a plausible TTI model, one must incorporate additional data or make additional assumptions. Another way to proceed is to analyze the null space of the solution using tomography with uncertainty analysis and to select anisotropic parameters based on a priori information from the area or rock-physics measurements.

Our study highlights challenges associated with TTI velocity model building from narrow-azimuth surveys. We expect wide-azimuth data to provide additional constraints and to reduce observed ambiguity for TTI models. We anticipate that this approach of well-constrained tomography can be applied to inversion for anisotropy in 2D and 3D TTI models and would allow anisotropic calibration with deviated wells.

ACKNOWLEDGMENTS

We thank Dmitry Alexandrov (summer intern from St. Petersburg State University) for help with generating the synthetic data set.

REFERENCES

Audebert, F. S., A. Pettenati, and V. Dirks, 2006, TTI anisotropic depth migration — Which tilt estimate should we use?: 68th Conference & Technical Exhibition, EAGE, Extended Abstracts, P185.

Bakulin, A., M. Woodward, D. Nichols, K. Osypov, and O. Zdraveva, 2009a, Localized anisotropic tomography with well information in VTI media: 79th Annual International Meeting, SEG, Expanded Abstracts, 221–225.

———, 2009b, Anisotropic model building with uncertainty analysis: 79th Annual International Meeting, SEG, Expanded Abstracts, 3720–3724.

Bear, L. K., T. A. Dickens, J. R. Krebs, J. Liu, and P. Traynin, 2005, Integrated velocity model estimation for improved positioning with anisotropic PSDM: The Leading Edge, **24**, 622–634.

Červený, V., 2001, Seismic ray theory: Cambridge University Press.

Chapman, C. H., and R. G. Pratt, 1992, Traveltime tomography in anisotropic media — I. Theory: Geophysical Journal International, **109**, 1–19.

Huang, T., S. Xu, and Y. Zhang, 2007, Anisotropy estimation for prestack depth imaging — A tomographic approach: 77th Annual International Meeting, SEG, Expanded Abstracts, 124–127.

Mateeva, A., A. Bakulin, P. Jorgensen, and J. Lopez, 2006, Accurate estimation of subsalt velocities using virtual checkshots: Offshore Technology Conference, Proceedings, OTC 17869.

Morice, S., J.-C. Puech, and S. Leaney, 2004, Well-driven seismic: 3D data processing solutions from wireline logs and borehole seismic data: First Break, **22**, 61–66.

Osypov, K., D. Nichols, M. Woodward, O. Zdraveva, and C. E. Yarman, 2008, Uncertainty and resolution analysis for anisotropic tomography using iterative eigendecomposition: 78th Annual International Meeting, SEG, Expanded Abstracts, 3244–3249.

Pech, A., I. Tsvankin, and V. Grechka, 2003, Quartic moveout coefficient: 3D description and application to tilted TI media: Geophysics, **68**, 1600–1610.

Pratt, R. G., and C. H. Chapman, 1992, Traveltime tomography in anisotropic media — II. Applications: Geophysical Journal International, **109**, 20–37.

Sengupta, M., R. Bachrach, and A. Bakulin, 2009, Relationship between velocity and anisotropy perturbations and anomalous stress field around salt bodies: The Leading Edge, **28**, 598–605.

Sexton, P., and P. Williamson, 1998, 3D anisotropic velocity estimation by model-based inversion of pre-stack traveltimes: 68th Annual International Meeting, SEG, Expanded Abstracts, 1855–1858.

Tsvankin, I., 2001, Seismic signatures and analysis of reflection data in anisotropic media: Elsevier Science Publ. Co., Inc.

Wang, X., and I. Tsvankin, 2009, Stacking-velocity tomography with borehole constraints for tilted TI media: 79th Annual International Meeting, SEG, Expanded Abstracts, 2352–2356.

Woodward, M., P. Farmer, D. Nichols, and S. Charles, 1998, Automated 3D tomographic velocity analysis of residual moveout in prestack depth migrated common image point gathers: 68th Annual International Meeting, SEG, Expanded Abstracts, 1218–1221.

Woodward, M., D. Nichols, O. Zdraveva, P. Whitfield, and T. Johns, 2008, A decade of tomography: Geophysics, **73**, no. 5, VE5–VE11.

Zhou, H., D. Pham, S. Gray, and B. Wang, 2004, Tomographic velocity analysis in strongly anisotropic TTI media: 74th Annual International Meeting, SEG, Expanded Abstracts, 2347–2350.